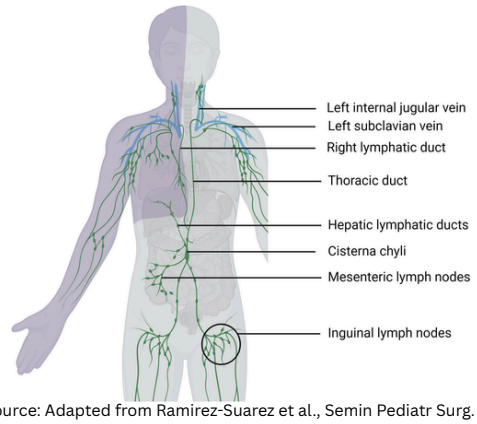
Lymphangiographic Anatomy for Intervention: A Practical Case-Based Pictorial Review

Dr. Janet Wong Hin Man, Dr. Alan YM Chong, Dr. Wisely HH Tang, Dr. John CY Chan, Dr. Dr. Kelvin KH Choi
Department of Radiology, Queen Mary Hospital

Introduction

The lymphatic system is a network of vessels found in multiple compartments of the body that allows for fluid balance, absorption of digested fats, and immune surveillance (1). There are three primary compartments: the soft tissue/peripheral lymphatics, the hepatic lymphatics, and the mesenteric lymphatics. These ultimately coalesce at the cisterna chyli which gives rise to the thoracic duct and drains into the central venous system. A separate right lymphatic duct drains the right upper extremity, right hemithorax, and right side of the head/neck (2). The main lymphovenous connection is between the thoracic duct and junction of the left subclavian and internal jugular veins with numerous additional normal lymphovenous connections in the body (3).

Lymphangiography has evolved from Kinmonth's pedal technique in 1955 to minimally invasive intranodal lymphangiography and selective lymphatic embolisation. Understanding normal lymphatic anatomy, flow pathways, and anatomical variation is therefore essential for image interpretation and procedural planning (4).

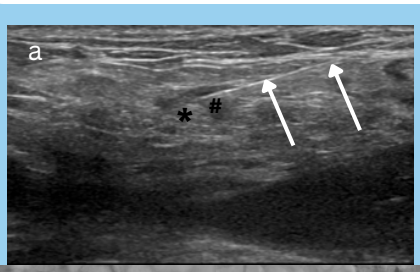


Source: Adapted from Ramirez-Suarez et al., Semin Pediatr Surg. 2024;33(3):151417. https://doi.org/10.1016/j.sempedsurg.2024.151417

Intra-nodal Access and Pelvis Ascent

Under ultrasound guidance, a superficial inguinal lymph node is accessed using a 23-25G needle positioned at the corticomedullary junction. Slow injection of Lipiodol opacifies the nodal medullary sinuses and ascends from the inguinal nodes through deep nodes and along the iliac chain toward the lumbar and cisterna chyli (2).

Fig. 1



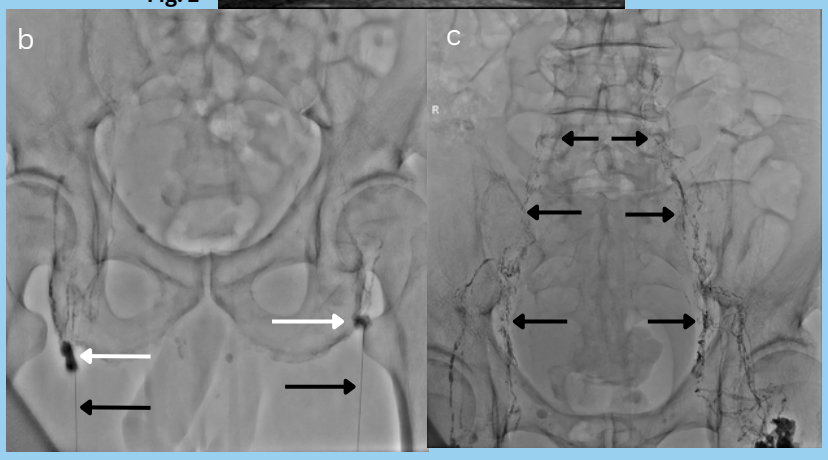


Figure 1. Intranodal access and antegrade pelvic lymphatic opacification.

(a) Under ultrasound guidance, a 25-gauge spinal needle (arrow) was inserted into a superficial inguinal lymph node, with the tip positioned at the corticomedullary junction between the hypoechoic cortex (#) and echogenic hilum (*). This positioning facilitates opacification of efferent lymphatic channels while reducing the risk of venous entry or capsular extravasation.

(b) AP fluoroscopic image following slow Lipiodol injection by spinal needles (black arrow) and nodal opacification at the inferomedial inguinal node (white arrow), near the level of the lesser trochanters.

(c) Serial fluoroscopic imaging demonstrates antegrade Lipiodol progression through the deep inguinal and iliac nodal chains into the lumbar (para-aortic) lymphatic channels (black arrows), illustrating the caudocranial route towards the central lymphatics.

Cisterna Chyli

The cisterna chyli (CC) is a sac-like dilatation of the lymphatic system deep within the retroperitoneum that is formed from lymphatic vessels that drain the abdominal, pelvis and lower limbs. The CC drains cranially into the thoracic duct. The prevalence of a discrete cisterna chyli is uncertain because of variable anatomical morphology and inconsistent definitions; reported rates range from approximately 50% in historic cadaveric studies.

Fig. 2

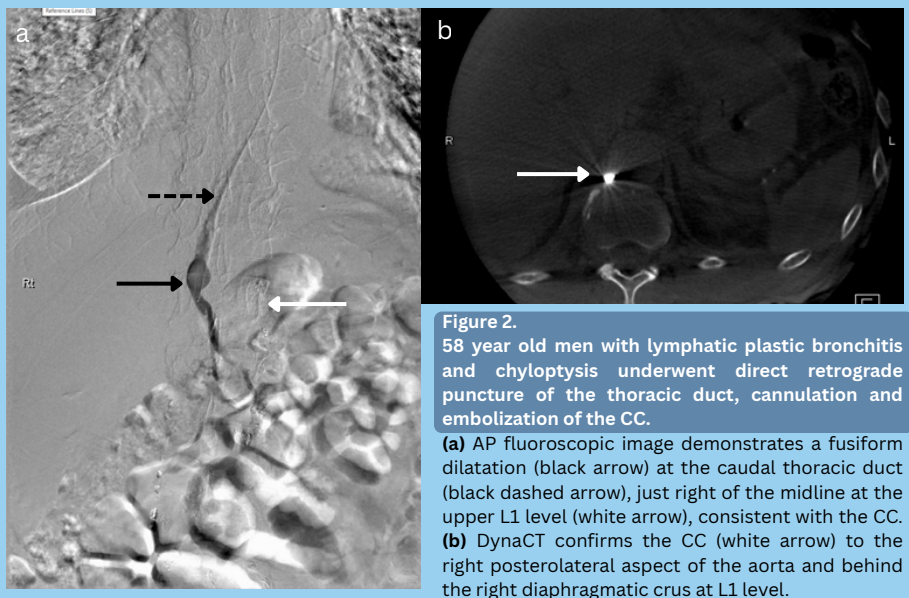


Figure 2.
58 year old men with lymphatic plastic bronchitis and chyloptysis underwent direct retrograde puncture of the thoracic duct, cannulation and embolization of the CC.
(a) AP fluoroscopic image demonstrates a fusiform dilatation (black arrow) at the caudal thoracic duct (black dashed arrow), just right of the midline at the upper L1 level (white arrow), consistent with the CC. **(b)** DynaCT confirms the CC (white arrow) to the right posterolateral aspect of the aorta and behind the right diaphragmatic crus at L1 level.

Its morphology is myriad, ranging from tubular or fusiform to saccular or plexiform. Its location is classically described as right of the midline at L1/L2 vertebral level, but it can be located midline, left sided or even rarely bilateral and retro-aortic. CC typically received lymph from the right and left lumbar trunks and the intestinal trunks (5).

Thoracic Duct

The CC drains into the thoracic duct (TD) which is the main lymphatic conduit, conveying lymph and chyle from the abdomen, pelvis, lower limbs, left hemithorax, left upper limb, and left head and neck into the systemic venous circulation. The thoracic duct typically enters the thorax via the aortic hiatus, coursing between the aorta and azygos vein. It usually crosses from right to left at the T5-T7 vertebral levels, then ascends into the lower neck (2-3cm above the clavicle) to terminate at confluence of the left internal jugular and subclavian veins, which is referred as the left venous angle (1).

It is estimated that the typical course of the thoracic duct is present in only 40–60 % of patients (6). Substantial variations are common, including complete right- or left-sided TD and CC, TD duplication (proximal or distal), plexiform configuration of lymphatic channels (7). These variants are relevant for interpretation of lymphangiograms and planning thoracic duct embolisation.

Cervical Thoracic Duct

The TD insertion point also demonstrates variable anatomy. Wirth and Kubik reported drainage of the thoracic duct into the left venous angle in 95% of cases, the right venous angle in 2%, and both venous angles in 3% (8). The exact point of entry into the venous system is also variable, a systematic review shows that the thoracic duct most commonly enters the internal jugular vein (46%), jugular venous angle (32%), subclavian vein (18%) and rarely other veins (4%). (9)

The terminal thoracic duct can be identified in up to 96% of patients on ultrasound and, when found, is almost always between the internal jugular vein and the left vertebral vein; rarely it passes posterior to the vertebral vein. (10)

Fig. 3

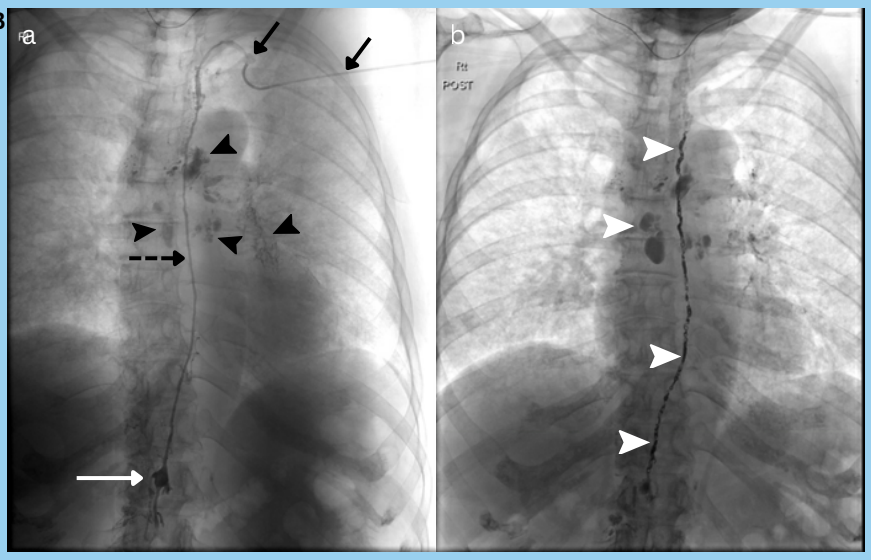


Figure 3. Left-sided thoracic duct and chylous pulmonary leakage in lymphatic plastic bronchitis.

A 76-year-old woman with lymphatic plastic bronchitis underwent right inguinal intranodal Lipiodol lymphangiography, followed by successful retrograde transvenous thoracic duct cannulation via left brachial venous access. **(a)** AP fluoroscopic image demonstrates the CC (white arrow) and a left-sided TD (black dashed arrow) ascending along the left aspect of the vertebral column throughout its course to the left venous angle. Mediastinal and bilateral hilar chylous leakage is evident (black arrowheads), consistent with abnormal pulmonary lymphatic perfusion underlying plastic bronchitis. Retrograde access through the left upper-extremity venous system enables catheterisation of the terminal thoracic duct at the lymphovenous junction (black arrow). **(b)** Thoracic duct embolisation was performed with microcoils followed by 50% NBCA–Lipiodol glue (white arrowheads).

Fig. 4

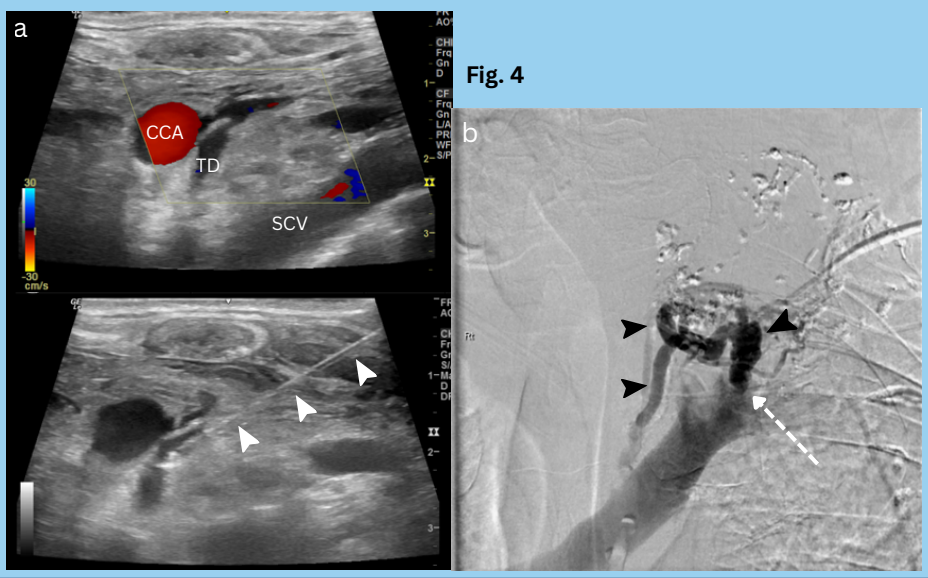


Figure 4. Direct ultrasound-guided retrograde cervical thoracic duct cannulation.

(a) Selected ultrasound images demonstrate percutaneous needle puncture (arrowheads) of the cervical thoracic duct (TD) in the left lower neck, with real-time identification of adjacent vascular structures including the common carotid artery (CCA) and subclavian vein (SCV). Ultrasound guidance enables direct puncture while avoiding arterial injury and confirms access to the tubular, non-vascular TD.

(b) Subsequent anteroposterior fluoroscopic image confirms contrast opacification of the cervical TD (white arrow) and its terminal drainage at the left jugulovenous angle (black arrowheads). Direct cervical TD access provides a retrograde route for thoracic ductography and embolisation, particularly when conventional transabdominal or transvenous cannulation is difficult.

Right Lymphatic Duct

The right lymphatic duct (RLD) is a short, approximately 1–2 cm terminal lymphatic channel that drains the right upper quadrant of the body, including the right hemithorax, right upper limb, right head and neck. It typically forms from the union of the right jugular, subclavian, and bronchomediastinal trunks and drains into the right venous angle at the confluence of the right internal jugular and subclavian veins, or brachiocephalic veins (7). This variability is clinically relevant in right lower-neck surgery and right-sided lymphatic interventions because unrecognised RLD injury can result in chylous leakage.

Fig. 5

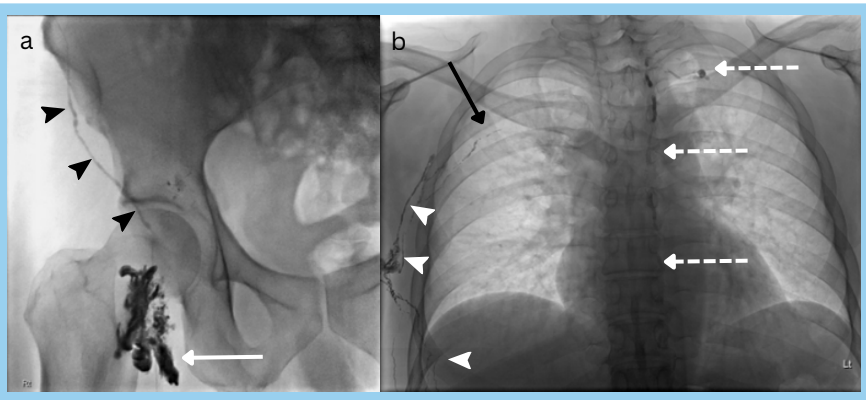


Figure 5. Retrograde superficial abdominal-wall lymphatic opacification with axillary drainage.

A 37 year old male with plastic bronchitis. Bilateral intra-nodal inguinal lymphangiogram was performed. **(a)** Following cannulation of a right inguinal lymph node (black arrow), there was retrograde opacification of superficial lymphatic channels in the infraumbilical anterior abdominal wall (black arrowheads). **(b)** Sequential fluoroscopic images demonstrated cephalad extension of Lipiodol across the transumbilical superficial lymphatic watershed, with drainage via right axillary lymphatic channels (white arrowheads), into the right lymphatic duct (black arrow). Traditional TD anatomy with cross to the left at mid-lower thoracic spine and drainage to left jugulovenous angle is also noted (white dash arrows).

Fig. 6

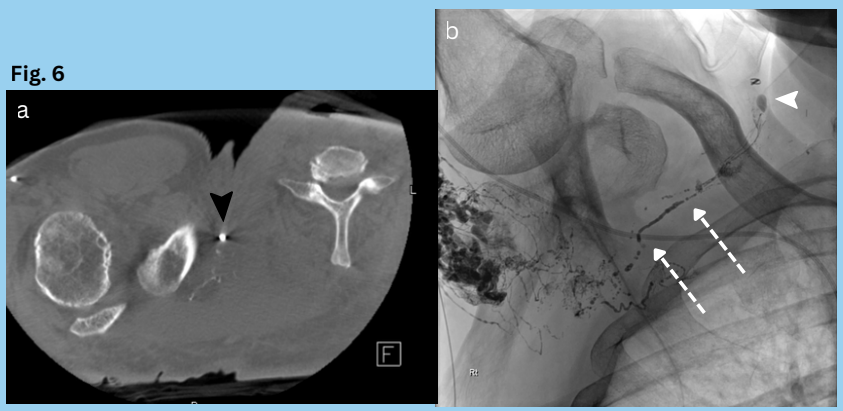


Figure 6. Right axillary intranodal lymphangiography and embolization of a postoperative cervical chyle leak.

A 67-year-old man with hypopharyngeal carcinoma developed a persistent right lower-neck collection following total laryngopharyngectomy with jejunal conduit and flap reconstruction. **(a)** Right axillary intranodal lymphangiography demonstrated contrast pooling in the right supraclavicular fossa; cone-beam CT (DynaCT) confirmed the site of lymphatic leakage (black arrowhead). **(b)** Embolization was performed with 2 mL of 33% NBCA–Lipiodol glue. Post-embolization fluoroscopy demonstrates a glue cast within the right-sided lymphatic duct and focal glue accumulation at the supraclavicular leak site, with subsequent cessation of leakage.

Fig. 7

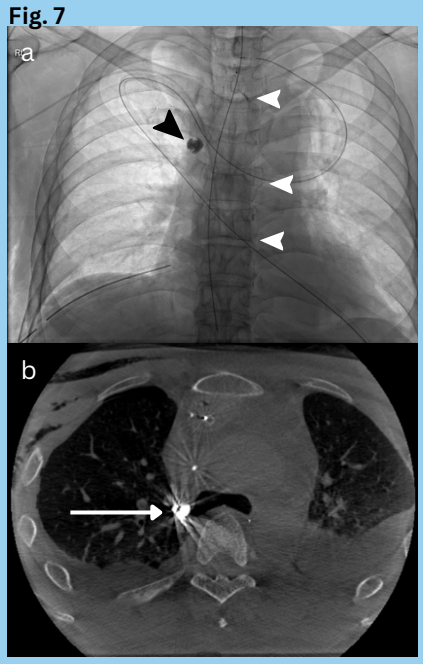


Figure 7. Incidental thoracic duct drainage into the azygos system.

A 53-year-old man with hypopharyngeal carcinoma following oesophagectomy, performed for persistent high-output postoperative pleural drainage. No active chylous leak was identified. **(a)** AP fluroscopic image showed conventional course of TD (white arrow heads) with Lipiodol uptake at right paravertebral region (black arrow head). **(b)** DynaCT confirmed Lipiodol uptake in the azygos vein (white arrow), representing a rare variant of thoracic duct with anomalous lymphovenous drainage into the azygos system.

Conclusion

Lymphatic intervention depends heavily on anatomy. Treatment success depends on ability to identify normal anatomy and thereby detecting abnormalities to guide intervention. Knowing the expected landmarks and variants can help guide interventional radiologists the right access route and correctly interpret findings.

The anatomy itself is still being defined. For decades, lymphatic imaging sat outside mainstream practice. Only in the last 20 years have intranodal and dynamic contrast-enhanced MR lymphangiography made it practical to show central lymphatic anatomy and disease in living patients (3). Even basic structures lack consistent definitions.

As newer interventions develop, including interstitial, hepatic and mesenteric lymphatic embolisation and lymphatic decompression, case-based anatomical atlases built from procedures will become more important for training and safe practice (3).

References

1. Understanding Lymphatic Anatomy and Abnormalities at Imaging Elizabeth Lee, David M. Biko, William Sherk, William R. Masch, Maria Ladino-Torres, and Prachi P. Agarwal RadioGraphics 2022 42:2, 487-505 10.1148/rg.210104
2. Important Anatomy in Lymphatic Interventions: A Practical Review Daniel A. Crawford, MD1 Indravadan J. Patel, MD1 Sailendra G. Naidu, MD1 Alex Wallace, MD1 Merve Ozen, MD1 Sadeer Alzubaidi, MD1 1Department of Radiology, Interventional Radiology, Mayo Clinic, Phoenix, Arizona
3. Imaging and Interventions for Lymphatic and Lymphatic-related Disorders. Jamaal Benjamin, Cathal O'Leary, Saebeom Hur, Alexey Gurevich, Willemijn M. Klein, and Maxim Itkin. Radiology 2023 307:3
4. Itkin, M., & Nadolski, G. J. (2018). Modern Techniques of Lymphangiography and Interventions: Current Status and Future Development. Cardiovascular and interventional radiology, 41(3), 366–376. https://doi.org/10.1007/s00270-017-1863-2
5. Moazzam S, O'Hagan LA, Clarke AR, et al. The cisterna chyli: a systematic review of definition, prevalence, and anatomy. Am J Physiol Heart Circ Physiol 323: H1010-H1018, 2022. doi: 10.1152/ajpheart.00375.2022.
6. Chen E, Itkin M (2011) Thoracic duct embolization for chylous leaks. Semin Interv Radiol 28:63–74
7. Johnson OW, Chick JFB, Chauhan NR, et al. The thoracic duct: clinical importance, anatomic variation, imaging, and embolization. European Radiology. 2016;26:2482–2493. doi:10.1007/s00330-015-4112-6.
8. Wirth W, Kubik S. Lymphographic roent-gen anatomy. In: Viamonte M, Ru¨ ttimannA, Agbaba M, eds. Atlas of lymphography.Stuttgart, Germany: Thieme-Verlag, 1980;71– 89
9. Phang K, Bowman M, Phillips A, Windsor J. Review of thoracic duct anatomical variations and clinical implications. Clin Anat. 2014;27(4):637–644. doi:10.1002/ca.22337
10. Seeger M, Bewig B, Günther R, et al. Terminal part of thoracic duct: high-resolution US imaging. Radiology 2009;252(03): 897–904